JVI Journals.ASM.org

# A Short Segment of the HIV-1 gp120 V1/V2 Region Is a Major Determinant of Resistance to V1/V2 Neutralizing Antibodies

**Nicole A. Doria-Rose,[a] Ivelin Georgiev,[a] Sijy O'Dell,[a] Gwo-Yu Chuang,[a] Ryan P. Staupe,[a] Jason S. McLellan,[a] Jason Gorman,[a] Marie Pancera,[a] Mattia Bonsignori,[b] Barton F. Haynes,[b] Dennis R. Burton,[c,d] Wayne C. Koff,[e] Peter D. Kwong,[a] and John R. Mascola[a]**

Vaccine Research Center, National Institute of Allergy and Infectious Diseases, National Institutes of Health, Bethesda, Maryland, USA[a]; Duke Human Vaccine Institute, Duke University School of Medicine, and Duke University Medical Center, Durham, North Carolina, USA[b]; Department of Immunology and Microbial Science and IAVI Neutralizing Antibody Center, The Scripps Research Institute, La Jolla, California, USA[c]; Ragon Institute of MGH, MIT, and Harvard, Cambridge, Massachusetts, USA[d]; and International AIDS Vaccine Initiative, New York, New York, USA[e]

**Antibody PG9 is a prototypical member of a class of V1/V2-directed antibodies that effectively neutralizes diverse strains of HIV-1. We analyzed strain-specific resistance to PG9 using sequence and structural information. For multiply resistant strains, mutations in a short segment of V1/V2 resulted in gain of sensitivity to PG9 and related V1/V2 neutralizing antibodies, suggesting both a common mechanism of HIV-1 resistance to and a common mode of recognition by this class of antibodies.**

Monoclonal antibodies (MAbs) capable of effectively neutralizing diverse strains of HIV-1 have been isolated from a number of HIV-1-infected individuals. One recently identified class of such antibodies recognizes an epitope primarily in the V1/V2 region of HIV-1 gp120, requires an N-linked glycan at residue 160, and generally binds with much higher affinity to membrane-associated trimeric forms of Env than to monomeric forms of gp120 (4, 15). Members of this class include PG9 and the somatically related PG16, as well as antibodies CH01 to CH04 and PGT141 to PGT145 from two other donors (1, 14, 15). Antibody PG9 is one of the most broadly cross-reactive members of the class and neutralizes 70 to 80% of diverse HIV-1 isolates (3, 7, 15). The structure of PG9 in complex with scaffolded forms of V1/V2 has been determined: when bound by PG9, V1/V2 adopts a 4-stranded β-sheet structure, with PG9 interacting with two glycans (at residues 156 and 160) and with one β-strand (strand C, at the sheet edge) (7). The free-antibody structures of PG9 as well as other antibodies from this class (PG16, CH04, and PGT145) are also known and suggest a common mode of Env recognition mediated primarily by the long anionic complementarity-determining region (CDR) H3 loops of these antibodies (7, 9, 10).

Previous studies indicated that virus neutralization sensitivity to PG9 might correlate with V2 length, the number and positioning of potential N-linked glycosylation sites in V1, V2, and V3, and net charge of the PG9-interacting strand C (2, 7, 11). Additionally, residues outside the structure-identified epitope—in V1/V2 as well as in V3—were found to affect PG9 and PG16 neutralization (8, 13, 15). Resistance conferred by an N160K mutation was described as a defining attribute for this class, but this residue does not account for all instances of resistance (15, 16). To gain a more complete understanding of the mechanism of naturally occurring viral resistance to PG9 and other MAbs of the class, we performed a combination of sequence and structural analyses to predict gain-of-sensitivity mutations among PG9-resistant strains. The effects of the mutations on resistance to PG9 and five other members of the V1/V2 antibody class were then assessed.

Among a panel of 172 HIV-1 Env pseudoviruses, 38 strains (22%) were found to be resistant to PG9 (3, 7). Examination of strain sequences indicated that 16 were missing the N-linked glycan at position 160, leaving a total of 134 sensitive and 22 resistant strains to be analyzed for protein sequence-based resistance signatures (Fig. 1). Initially, we focused on residues 154 to 184 of V1/V2 (HXB2-relative residue numbering), a region that spans β-strands B and C, is relatively conserved (with few insertions/deletions), and includes the entire PG9 epitope (7). Specifically, based on sequence alignments, we searched for amino acids that were preferentially found among PG9-resistant versus -sensitive

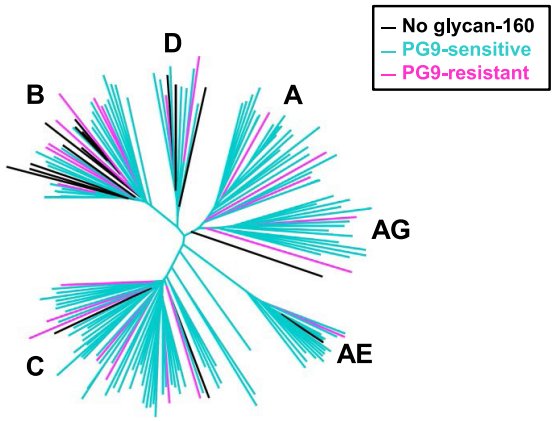


**FIG 1** PG9 neutralization sensitivity and resistance. Neighbor-joining dendrogram constructed from full gp160 sequences of 172 virus strains representing the major HIV-1 genetic subtypes (labeled branches). Neutralization sensitivity of each Env pseudovirus is indicated by the color of the branch: PG9-resistant strains not containing a PNGS at residue 160 are in black, PG9-sensitive strains are in aqua, and all other PG9-resistant strains are in pink.

**Received** 20 April 2012 **Accepted** 9 May 2012
**Published ahead of print** 23 May 2012
Address correspondence to Peter D. Kwong, pkwong@mail.nih.gov, or John R. Mascola, jmascola@mail.nih.gov.
N.A.D.-R. and I.G. contributed equally to this work.
Supplemental material for this article may be found at http://jvi.asm.org.

doi:10.1128/JVI.00696-12

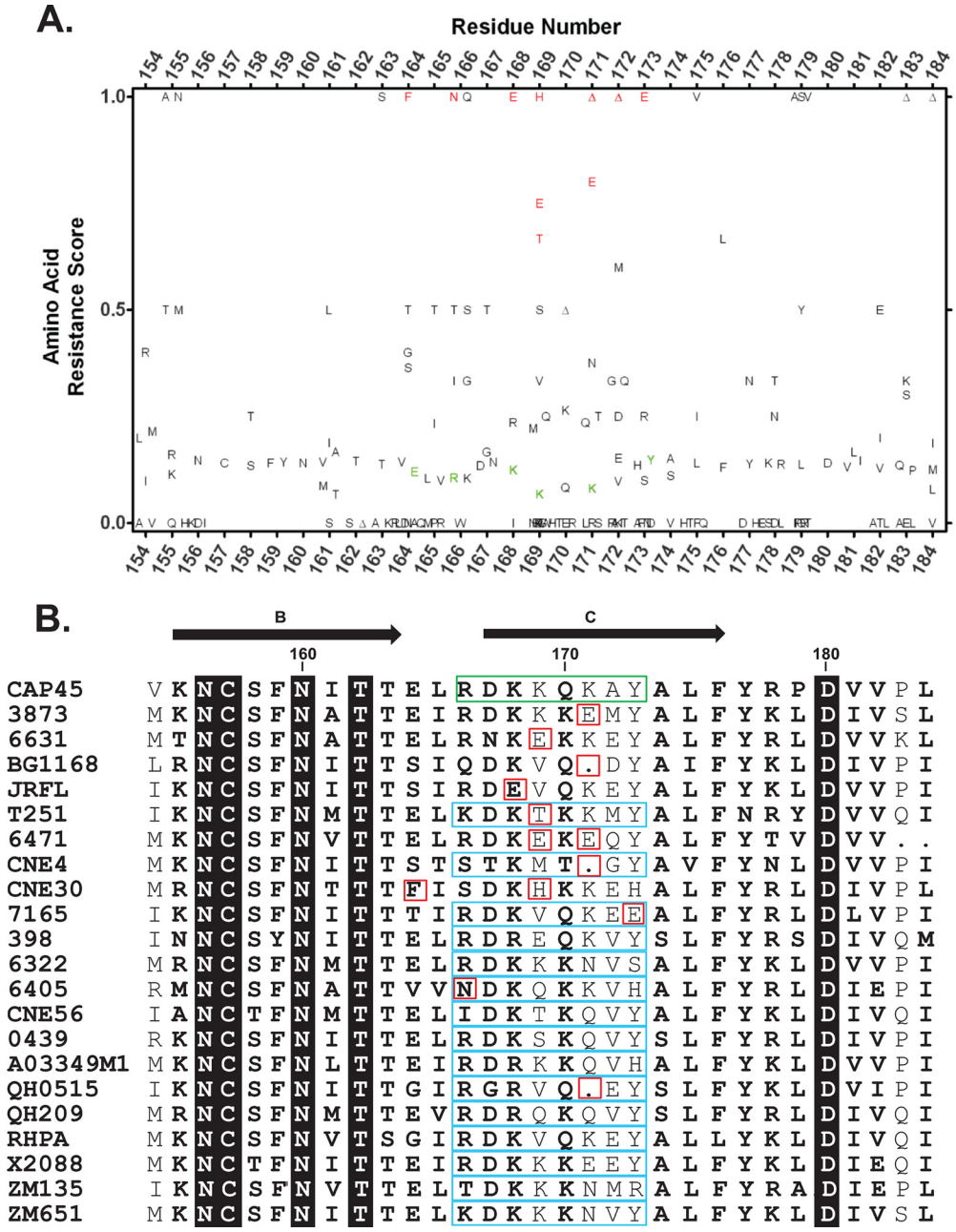


**FIG 2** Design of gain-of-sensitivity mutants among PG9-resistant strains. (A) V1/V2 amino acid frequency analysis. Symbols correspond to the respective amino acids, with △ representing sequence gaps at the given position. For each residue at positions 154 to 184 (HXB2-relative numbering), the resistance score for a given amino acid (or a gap) was defined as the ratio of its number of occurrences in resistant sequences to its overall number of occurrences for the given residue position. A higher score indicates that the amino acid was preferentially found among resistant sequences, with a score of 1 indicating that the amino was found only among resistant sequences. Residues highlighted in red were selected for gain-of-sensitivity studies and were mutated to the amino acid types shown in green for the specified residue positions. (B) PG9-resistant strains selected for gain-of-function experiments, with highlighted residues selected for point-mutations (red) and/or swaps (cyan). The PG9-sensitive CAP45 sequence, used to determine the atomic structure of V1/V2, is shown as a reference, with the residue segment used in the swaps with the resistant strains highlighted in green. Strands B and C of V1/V2 shown at the top of the figure are based on the CAP45 structure. Residue positions with no variation are shown in white font on black background, while conserved residue positions are shown in bold.

strains for a given residue position (Fig. 2A). A number of such amino acids at positions at or near the PG9 interface (as observed in the crystal structure of scaffolded V1/V2) were selected for gain-of-sensitivity mutations (Fig. 2B). Each of the selected residues was mutated to amino acids commonly observed among PG9-sensitive sequences (Fig. 2A). This sequence analysis was able to identify candidate mutations for 11 of the PG9-resistant strains. However, since the selected mutations were primarily in the short segment between residues 166 and 173, which overlaps strand C of V1/V2, we swapped that 8-residue segment in 10 additional strains, as well as in five of the strains identified by the sequence analysis, with the corresponding segment from CAP45, a sensitive

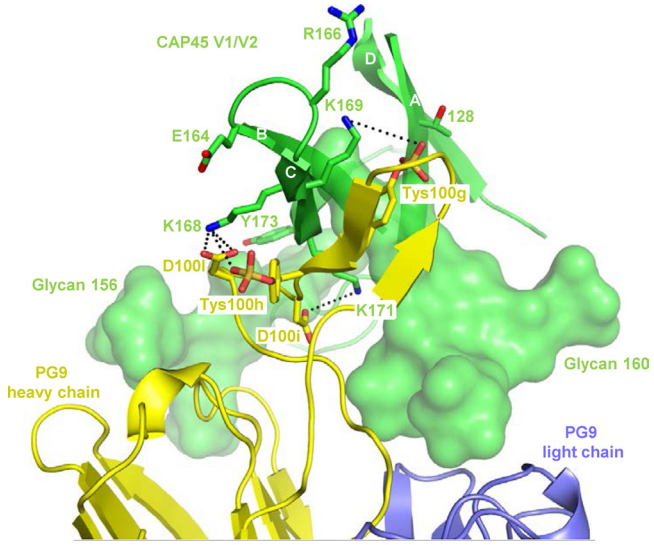


**FIG 3** Structure-based explanation of gain-of-sensitivity results for V1/V2-directed broadly neutralizing antibodies. The structure of scaffolded V1/V2 from the CAP45 strain of HIV-1 (green ribbon with labeled strands and molecular surfaces of glycans 156 and 160) is shown in complex with PG9 (yellow, heavy chain; blue, light chain). The side chains of V1/V2 residues selected for gain-of-sensitivity mutation are shown as sticks and labeled by residue number; side chains of proximal interacting residues in PG9 CDR H3 are shown as yellow sticks and labeled.

strain used for the PG9 crystal structure (7) (Fig. 2B). Additionally, analysis of potential N-linked glycosylation sites (PNGS) revealed that residue 128 was the location of a PNGS in the PG9-resistant strain CNE4 but not in any of the other strains in the neutralization panel. Since glycans may create substantial steric hindrance, PNGS 128 in CNE4 was also selected for gain-of-sensitivity experiments, despite a more distal position with respect to the PG9 interface in the scaffolded V1/V2 structures (Fig. 3).

In total, 21 PG9-resistant HIV-1 isolates (three from clade A, six from B, seven from C, two from D, and one each from AE, AG, and G) were analyzed by mutagenesis and neutralization assays (Table 1; also, see Table S1 in the supplemental material). The point mutations and strand C swaps were generated by site directed mutagenesis (GeneImmune LLC, New York, NY) on Env expression plasmids (5, 6, 15, 17). Parental and mutant Envs were used to construct pseudoviruses for the single round of infection neutralization assays using TZM-bl target cells as described previously (12, 17). Each pair of parental and mutant viruses was tested against six members of the V1/V2-directed class of broadly neutralizing antibodies, isolated from three different donors: PG9 and PG16 (15), CH01 and CH04 (1), and PGT141 and PGT145 (14). In each case, the parental virus was resistant to PG9 at a 50% inhibitory concentration ($IC_{50}$) of >50 μg/ml, although several were sensitive to other V1/V2 MAbs. MAbs to other epitopes (MAbs VRC01, F105, 17b, PGT128, and 4E10) were included as controls to assess the impact of the mutations on overall Env conformation and neutralization sensitivity.

Mutations that changed the glutamic acid (E) to lysine (K) at position 168, 169, or 171 had the most dramatic effects on sensitivity to the V1/V2 MAbs (Table 1; also, see Table S1 in the supplemental material). For viral strains 3873, 6631, BG1168, JRFL, and T251, a single point mutation at one of these three sites was sufficient to confer sensitivity to multiple V1/V2 MAbs. For resistant strain 6471, the double mutation E169K/E171K resulted in neutralization sensitivity to all six V1/V2 MAbs tested. Point mutations had a more modest effect on some viral strains: CNE4 with an inserted 171K gained sensitivity to just PG9, and CNE30-F164E/H169K gained sensitivity to both PG9 and PG16 but no others.

These observations confirm and extend the information gained from the crystal structures of PG9 with scaffolded V1/V2 from strains ZM109 and CAP45 (7). In these structures, V1/V2 residues 168, 169, and 171 are part of the cationic V1/V2 strand C that interacts directly with a number of negatively charged residues in the CDRH3 of PG9: sulfated tyrosines Tys 100g and Tys 100h and Asp 100i and Asp 100l (Kabat residue numbering). Negatively charged residues and deletions at positions 168, 169, and 171 likely disturb interactions and/or create charge repulsion with PG9 CDRH3 (Fig. 3). This interpretation is consistent with a recent study showing a correlation of net positive charge in V2 strand C with sensitivity to PG9 and PG16 (11). Similarly, mutagenesis studies have found that K169E confers resistance to PG9 and PG16, while the less drastic K171A mutation had a more moderate effect on neutralization by these antibodies (8, 13, 15).

Additional positions in strand C also affected sensitivity to V1/V2 antibodies. The E173Y mutation in 7165 effectively conferred sensitivity, in agreement with previous results showing loss of neutralization of Y173A in JR-CSF for both PG9 and PG16 (15). E173Y could potentially stabilize the positioning of glycan-156 and may thus have an indirect effect on interactions with PG9 (Fig. 3), though the mechanism of action of this mutation is less clear than that of the 168, 169, and 171 mutations.

Replacement of an 8-residue segment (residues 166 to 173, overlapping strand C) with the corresponding segment from CAP45 also conferred complete V1/V2 MAb sensitivity to strains 398, 6322, 6405, and CNE56. Sensitivity to at least one MAb, including PG9, was observed for the CAP45 C-strand chimeras of 0439, A03349M1, QH0515, QH209, RHPA, X2088, ZM135, and ZM651. For three of the strains for which both point mutants and CAP45 C-strand chimeras were tested, the strand C swap had the more dramatic effect. Strain CNE4 was resistant to all six MAbs, the PNG removal mutant CNE4-N128T.T130D had no effect on neutralization resistance, and CNE4-ins171K gained sensitivity only to PG9, but the CAP45 strand-C chimera was sensitive to PG9, PG16, and CH01. Similarly, on strain 6405, the point mutant N166R only gained sensitivity to PGT141, possibly indicating additional interactions with the longer PGT141 penetrating loop (7, 14), which may extend further toward the 166 region than that of PG9 (Fig. 3). In contrast, the CAP45 strand C swap provided sensitivity to all six MAbs. Finally, the point mutation in QH0515-ins171K had no effect on sensitivity, but the CAP45 strand C chimera conferred PG9 neutralization.

Paradoxically, in four cases, while the CAP45 strand C chimeras gained sensitivity to PG9 and PG16, a gain of resistance was noted for CH01 and CH04 (strain T251), PGT141 (RHPA and 7165), and PGT145 (QH209). This observation suggests that, despite overall similarity in the epitope recognized and the requirement for the N160 glycan, there is some variation in the mode of recognition by members of the V1/V2 class of neutralizing MAbs.

The mutations tested here did not cause global alterations in the neutralization sensitivity as assessed by MAbs to non-V1V2 epitopes (Table 1; also, see Table S1 in the supplemental material).

**TABLE 1** Neutralization $IC_{50}$s for 21 PG9-resistant HIV-1 Env pseudoviruses and their corresponding gain-of-function mutants

| Clade | Virus[a] | $IC_{50}$ (μg/ml)[b] | | | | | | | | | | |
|---|---|---|---|---|---|---|---|---|---|---|---|---|
| | | V1/V2 MAbs | | | | | | Control MAbs[c] | | | | |
| | | PG9 | PG16 | CH01 | CH04 | PGT141 | PGT145 | VRC01 | F105 | 17b | PGT128 | 4E10 |
| C | 3873 | >50 | >50 | >50 | >50 | **0.011** | **0.009** | **0.475** | >50 | >50 | **0.006** | **6.43** |
| | 3873-E171K | **0.018** | **0.004** | **0.161** | **0.385** | **0.003** | **0.004** | **0.071** | >50 | >50 | **0.006** | **2.75** |
| C | 6631 | >50 | >50 | >50 | >50 | >50 | >50 | >50 | >50 | >50 | **4.07** | >50 |
| | 6631-E169K | **0.225** | **0.047** | **1.66** | **0.759** | **12.3** | >50 | >50 | >50 | >50 | **4.52** | >50 |
| B | BG1168 | >50 | >50 | >50 | >50 | >50 | >50 | **0.203** | >50 | >50 | >50 | **1.84** |
| | BG1168-ins171K | **4.99** | **0.276** | >50 | >50 | >50 | **0.517** | **0.670** | >50 | >50 | >50 | **5.15** |
| B | JRFL | >50 | >50 | >50 | >50 | >50 | **8.77** | **0.029** | >50 | >50 | **0.01** | **6.16** |
| | JRFL-E168K | **0.009** | **<0.003** | **0.122** | **0.095** | **0.11** | **0.017** | **0.023** | >50 | >50 | **0.006** | **4.04** |
| AG | T251 | >50 | **5.23** | **13.6** | **29.5** | >50 | **0.316** | **3.03** | >50 | >50 | >50 | **10.3** |
| | T251-T169K | **0.056** | **0.022** | **2.51** | **3.67** | >50 | **0.059** | **2.85** | >50 | >50 | >50 | **7.01** |
| | T251-C[d] | **0.210** | **0.104** | >50 | >50 | **0.009** | **0.038** | **3.35** | >50 | >50 | >50 | **16.8** |
| C | 6471 | >50 | >50 | >50 | >50 | >50 | >50 | >50 | >50 | >50 | >50 | >50 |
| | 6471-E169K/E171K | **0.045** | **0.012** | **1.32** | **1.32** | **0.043** | **0.080** | >50 | >50 | >50 | >50 | **8.57** |
| B | CNE4 | >50 | >50 | >50 | >50 | >50 | >50 | **0.352** | **17.9** | **18.1** | **0.546** | **0.822** |
| | CNE4-N128T/T130D | >50 | >50 | >50 | >50 | >50 | >50 | **0.165** | **0.554** | **15.6** | **2.02** | **0.17** |
| | CNE4-ins171K | **0.312** | >50 | >50 | >50 | >50 | >50 | **0.266** | **0.236** | **0.214** | >50 | **0.043** |
| | CNE4-C | **0.049** | **15.9** | **36.5** | >50 | >50 | >50 | **0.321** | **0.338** | **0.198** | >50 | **0.135** |
| C | CNE30 | >50 | >50 | >50 | >50 | >50 | >50 | **0.979** | >50 | >50 | **0.19** | **4.70** |
| | CNE30-F164E | >50 | >50 | >50 | >50 | >50 | >50 | **0.714** | >50 | >50 | **0.417** | **13.4** |
| | CNE30-F164E/H169K | **2.37** | **0.648** | >50 | >50 | >50 | >50 | **0.686** | >50 | >50 | **0.255** | **9.51** |
| B | 7165 | >50 | >50 | >50 | >50 | **2.15** | **0.063** | **26.6** | >50 | >50 | **0.004** | **1.79** |
| | 7165-E173Y | **0.603** | **0.045** | **1.07** | **2.45** | **0.151** | **0.029** | >50 | >50 | >50 | **0.004** | **3.21** |
| | 7165-C | **0.020** | **0.008** | **0.209** | **0.608** | >50 | 0.031 | >50 | >50 | >50 | **<0.003** | **1.75** |
| A | 398 | >50 | >50 | **0.266** | **0.463** | >50 | >50 | **0.144** | >50 | >50 | **<0.003** | **8.56** |
| | 398-C | **0.004** | **0.003** | **0.059** | **0.095** | **0.144** | **0.38** | **0.081** | >50 | >50 | **<0.003** | **0.329** |
| C | 6322 | >50 | >50 | >50 | >50 | **0.013** | **0.105** | >50 | >50 | >50 | >50 | **11.4** |
| | 6322-C | **0.019** | **0.008** | **0.696** | **1.14** | **<0.003** | **<0.003** | >50 | >50 | >50 | >50 | **7.10** |
| D | 6405 | >50 | >50 | >50 | >50 | >50 | >50 | **1.53** | >50 | >50 | **3.86** | **9.10** |
| | 6405-N166R | >50 | >50 | >50 | >50 | **1.27** | >50 | **1.39** | >50 | >50 | **2.82** | **4.17** |
| | 6405-C | **0.245** | **0.195** | **2.05** | **6.39** | **0.004** | **0.117** | **0.815** | >50 | >50 | **3.64** | **1.34** |
| AE | CNE56 | >50 | >50 | >50 | >50 | >50 | **2.25** | **0.186** | >50 | >50 | **7.36** | **0.960** |
| | CNE56-C | **0.165** | **0.033** | **2.79** | **2.93** | **0.128** | **0.807** | **0.341** | >50 | >50 | **2.03** | **0.219** |
| A | 0439 | >50 | >50 | >50 | >50 | **3.91** | **2.00** | **0.170** | >50 | >50 | **2.57** | **6.70** |
| | 0439-C | **4.19** | >50 | >50 | >50 | **1.54** | **2.76** | **0.116** | >50 | >50 | **2.58** | **2.50** |
| D | A03349M1 | >50 | >50 | >50 | >50 | >50 | **2.71** | **2.83** | >50 | >50 | **0.01** | **4.60** |
| | A03349M1-C | **1.18** | **0.181** | >50 | >50 | **0.937** | **0.059** | **0.637** | **10.4** | >50 | **0.012** | **1.27** |
| B | QH0515 | >50 | >50 | >50 | >50 | >50 | >50 | **0.11** | >50 | >50 | >50 | **3.07** |
| | QH0515-ins171K | >50 | >50 | >50 | >50 | >50 | >50 | **0.769** | >50 | >50 | >50 | **3.59** |
| | QH0515-C | **4.58** | >50 | >50 | >50 | >50 | >50 | **1.19** | >50 | >50 | >50 | **1.65** |
| A | QH209 | >50 | >50 | >50 | >50 | >50 | **0.015** | **0.017** | >50 | >50 | >50 | **5.27** |
| | QH209-C | **0.39** | **0.124** | >50 | >50 | >50 | >50 | **0.025** | >50 | >50 | >50 | **4.81** |
| B | RHPA | >50 | **0.816** | >50 | **34.4** | **0.064** | **0.044** | **0.035** | >50 | >50 | **0.010** | **5.66** |
| | RHPA-C | 0.603 | **0.101** | **7.78** | **38.5** | >50 | **2.48** | **0.031** | >50 | >50 | **0.008** | **5.03** |

(Continued on following page)

**TABLE 1** (Continued)

| Clade | Virus[a] | $IC_{50}$ (μg/ml)[b] | | | | | | | | | | |
|---|---|---|---|---|---|---|---|---|---|---|---|---|
| | | V1/V2 MAbs | | | | | | Control MAbs[c] | | | | |
| | | PG9 | PG16 | CH01 | CH04 | PGT141 | PGT145 | VRC01 | F105 | 17b | PGT128 | 4E10 |
| G | X2088 | >50 | >50 | >50 | >50 | >50 | >50 | >50 | >50 | >50 | >50 | >50 |
| | X2088-C | **0.11** | **0.694** | >50 | >50 | >50 | >50 | >50 | >50 | >50 | >50 | >50 |
| C | ZM135 | >50 | >50 | >50 | >50 | >50 | >50 | **0.237** | >50 | >50 | **3.92** | **0.136** |
| | ZM135-C | **0.099** | **0.03** | >50 | >50 | **0.004** | **0.148** | **1.19** | >50 | >50 | **5.68** | **0.746** |
| C | ZM651 | >50 | >50 | >50 | >50 | >50 | **7.56** | **0.558** | >50 | >50 | **0.101** | **0.462** |
| | ZM651-C | **22.5** | >50 | >50 | >50 | **2.93** | **8.22** | **1.3** | >50 | >50 | >50 | **1.38** |

[a] Strains marked with C have the CAP45 strand C swap as described in the text. Full names of strains are provided in Table S1 in the supplemental material.
[b] A value of >50 indicates no neutralization at 50 μg/ml. All other values are in bold. $IC_{80s}$ are reported in Table S1.
[c] Control MAb epitopes: VRC01 and F105, CD4 binding site; 17b, CD4 induced; PGT128, glycan/loop; 4E10, membrane-proximal region.

The one exception was strain CNE4, for which the mutants increased accessibility to the CD4 binding site (targeted by control MAb F105) and CD4-induced epitopes (targeted by 17b) while decreasing the potency of PGT128 (glycans). The other 20 strains showed little change in sensitivity to the control MAbs, indicating that the effects of the mutations were likely specific for V1/V2 recognition.

These gain-of-sensitivity mutational analyses support the conclusions drawn from the scaffolded V1/V2-PG9 crystal structures, suggesting that the conformations observed for these engineered constructs are biologically and functionally relevant. For each of the PG9-resistant strains selected for gain-of-function experiments, at least one of the selected mutants gained sensitivity to one or more of the V1/V2 MAbs, thus validating the predictions based on structure and sequence. While correlations of PG9 resistance with other factors such as glycosylation and length of V2 have also been noted, our results suggest a general mechanism of resistance to V1/V2-directed broadly neutralizing antibodies that involves alteration of basic residues within strand C of the V1/V2 domain. Additionally, our observation that gain-of-sensitivity mutations generally affected not only PG9 but also antibodies PG16, CH01, CH04, PGT141, and PGT145 provides further evidence that the members of this class recognize a similar epitope on the native HIV-1 envelope glycoprotein.

## ACKNOWLEDGMENTS

Support for this work was provided by the Intramural Research Program of the Vaccine Research Center, NIAID, NIH, by the Center for HIV/AIDS Vaccine Immunology (CHAVI) grant AI067854 from the Division of AIDS, NIAID, NIH, by grant AI 033292 from NIAID, NIH, and by the International AIDS Vaccine Initiative.

We are grateful to Brenda Hartman for assistance with graphics. We thank members of the Structural Biology Section, Structural Bioinformatics Core, Humoral Immunity Section, and BSL-3 Core at the NIH Vaccine Research Center for helpful discussions of the manuscript.

## REFERENCES

1. **Bonsignori M, et al.** 2011. Analysis of a clonal lineage of HIV-1 envelope V2/V3 conformational epitope-specific broadly neutralizing antibodies and their inferred unmutated common ancestors. J. Virol. **85**:9998–10009.
2. **Doores KJ, Burton DR.** 2010. Variable loop glycan dependency of the broad and potent HIV-1-neutralizing antibodies PG9 and PG16. J. Virol. **84**:10510–10521.
3. **Doria-Rose NA, et al.** 2012. HIV-1 neutralization coverage is improved by combining monoclonal antibodies that target independent epitopes. J. Virol. **86**:3393–3397.
4. **Kwong PD, Mascola JR, Nabel GJ.** 2009. Mining the B cell repertoire for broadly neutralizing monoclonal antibodies to HIV-1. Cell Host Microbe **6**:292–294.
5. **Li M, et al.** 2005. Human immunodeficiency virus type 1 *env* clones from acute and early subtype B infections for standardized assessments of vaccine-elicited neutralizing antibodies. J. Virol. **79**:10108–10125.
6. **Li M, et al.** 2006. Genetic and neutralization properties of subtype C human immunodeficiency virus type 1 molecular *env* clones from acute and early heterosexually acquired infections in Southern Africa. J. Virol. **80**:11776–11790.
7. **McLellan JS, et al.** 2011. Structure of HIV-1 gp120 V1/V2 domain with broadly neutralizing antibody PG9. Nature **480**:336–343.
8. **Moore PL, et al.** 2011. Potent and broad neutralization of HIV-1 subtype C by plasma antibodies targeting a quaternary epitope including residues in the V2 loop. J. Virol. **85**:3128–3141.
9. **Pancera M, et al.** 2010. Crystal structure of PG16 and chimeric dissection with somatically related PG9: structure-function analysis of two quaternary-specific antibodies that effectively neutralize HIV-1. J. Virol. **84**:8098–8110.
10. **Pejchal R, et al.** 2010. Structure and function of broadly reactive antibody PG16 reveal an H3 subdomain that mediates potent neutralization of HIV-1. Proc. Natl. Acad. Sci. U. S. A. **107**:11483–11488.
11. **Ringe R, Phogat S, Bhattacharya J.** 2012. Subtle alteration of residues including N-linked glycans in V2 loop modulate HIV-1 neutralization by PG9 and PG16 monoclonal antibodies. Virology. **426**:34–41.
12. **Shu Y, et al.** 2007. Efficient protein boosting after plasmid DNA or recombinant adenovirus immunization with HIV-1 vaccine constructs. Vaccine. **25**:1398–1408.
13. **Thenin S, et al.** 2012. Naturally occurring substitutions of conserved residues in HIV-1 variants of different clades are involved in PG9 and PG16 resistance to neutralization. J. Gen. Virol. [Epub ahead of print.] doi:10.1099/vir.0.042614-0.
14. **Walker LM, et al.** 2011. Broad neutralization coverage of HIV by multiple highly potent antibodies. Nature **477**:466–470.
15. **Walker LM, et al.** 2009. Broad and potent neutralizing antibodies from an African donor reveal a new HIV-1 vaccine target. Science **326**:285–289.
16. **Wu X, et al.** 2011. Immunotypes of a quaternary site of HIV-1 vulnerability and their recognition by antibodies. J. Virol. **85**:4578–4585.
17. **Wu X, et al.** 2010. Rational design of envelope identifies broadly neutralizing human monoclonal antibodies to HIV-1. Science **329**:856–861.